

Deep Reinforcement Learning based Blind mmWave MIMO Beam Alignment

Vishnu Raj Sheetal Kalyani

Department of Electrical Engineering,
Indian Institute of Technology Madras,
Chennai, India, 600 036.

{ee14d213, skalyani}@ee.iitm.ac.in

Abstract—Directional beamforming is a crucial component for realizing robust wireless communication systems using millimeter wave (mmWave) technology. Beam alignment using brute-force search of the space introduces time overhead while location aided blind beam alignment adds additional hardware requirements to the system. In this paper, we introduce a method for blind alignment based on the RF fingerprints of user equipment obtained by the base stations. The proposed system performs blind beamforming on a multiple base station cellular environment with multiple mobile users using deep reinforcement learning. We present a novel neural network architecture that can handle a mix of both continuous and discrete actions and use policy gradient methods to train the model. Our results show that the proposed model is able to give a considerable improvement in data rates over traditional methods.

Index Terms—MIMO, Beam Alignment, Deep Reinforcement Learning

I. INTRODUCTION

Millimeter Wave (mmWave) communication systems are considered as one of the key technologies in next-generation wireless systems. Massive MIMO systems with mmWave technologies combine the advantages of leveraging spatial resources of MIMO with the high data rates offered by the large bandwidth available at millimeter wave frequency bands. However, excessive pathloss and penetration loss incurred during wave propagation severely affect the range of mmWave MIMO systems. Directional transmission and antenna beamforming have been proposed as a solution for compensating for the losses incurred during wave propagation [1].

Directional beamforming has been traditionally achieved through beam sweeping methods [2], which involves a brute-force search through the possible steering directions. But this brute-force search method is both time consuming and puts additional load on the energy expenditure. To reduce the complexity of the full scale search, hierarchical search strategies have been proposed (See [3] and references therein). Blind beam steering relying on accurate location information has been proposed as a low complexity solution for beamforming [4], but comes with the overhead of additional location information. In a recent work, [5] develops a method based on Extended Kalman Filter to track the mmWave beam in a mobile scenario with moving UEs.

The progress in deep learning in the areas of computer vision and speech signal processing [6] has also triggered an interest

in applying those techniques to complex wireless communication problems [7]. Deep learning has been successfully used in channel estimation [8], end to end communication systems [9], [10], OFDM systems [11] etc. Application of developments in deep learning research has also improved the solutions for mmWave communication systems. Some of the fruitful applications include beamforming design for weighted sum-rate maximization [12], using an autoencoder deep learning model to improve hybrid precoding [13], replacing hybrid precoding with a deep learning model to predict the best pair transmit/receive beampairs from the observed channel [14] and leveraging deep reinforcement learning for beamforming [15]. It can be observed from these works that mmWave MIMO systems can greatly benefit from the application of learning techniques into its core components.

In this work, we consider the problem of blind mmWave beam alignment in a downlink channel using only the RF signature about the presence of UE in the system. Specifically, we consider a multi-base station (BS) scenario with multiple mobile users (UE). A simple depiction of the scenario is given in Fig. 1.

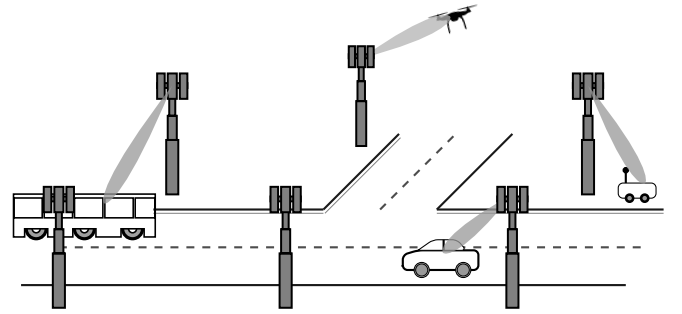


Fig. 1: A depiction of problem scenario

We consider a scenario where multiple mmWave micro basestations (μ BS) exist and there is a central basestation (not depicted in Fig. 1) which co-ordinates all the transmissions μ BS. Due to the pathloss and penetration loss properties of mmWave, each μ BS has only limited coverage area, usually within hundreds of meters. As the mobile users move in the environment, we need to select the best μ BS to serve each user based on the channel characteristics between μ BS and users. These user equipments can be any mobile transmitter which

employs mmWave for communication. Examples of such user terminals include mobile phones, connected vehicles, autonomous cars, delivery robots, unmanned aerial vehicles (UAVs) etc. Specifically, our aim is to select one μ BS out of the available basestations to serve each user and also to find the best beam alignment angles for transmission without any brute-force beam sweep methods. Rather than relying on the location information for beam alignment as considered in previous works, the proposed method uses radio frequency (RF) signature available in the system about the presence of the UEs and leverage the advancements in deep reinforcement learning to achieve blind beam alignment from BS to UE for downlink communication.

Related Works. Deep learning based solutions for beam alignment with no location information have been proposed under multiple scenarios. In [16], a coordinated beamforming solution using deep learning to enable high mobility and high data rate is proposed. Based on the uplink pilot signal received at the terminal BSs, a deep neural network is trained to predict the best beam forming vectors. The method is applied to the scenario where multiple BSs serve a single UE. Extending this method to support multiple UEs may not control the interference between the UEs as the existence of multiple UEs is not known to the trained deep learning model. Another approach that takes into account the varying traffic patterns and its impact on the mmWave channel is proposed in [17]. By taking location, traffic parameters and RSSI thresholds of each UE, the proposed method suggests a set of beamforming vector based on an estimated RF fingerprint which can then be used to do conduct beam training. By deploying a deep learning based method to shortlist possible best beamforming vectors, this method can reduce the beam training time for initiating an mmWave communication. However, to train this model, an exhaustive dataset of possible RF fingerprints across multiple traffic patterns is required. On the other side, once trained, the model can continue to operate as long as there is no major change in the environment. In an alternative take on the problem, [18] proposed a solution that includes BSs broadcasting its location. UEs (connected vehicles with LIDARs) fuses the information from its LIDAR and the received BS location information to shortlist a possible set of beamforming vectors. This also helps in reducing the delay due to brute force beam search. The work in [19] proposed to use the LIDAR in connected smart vehicles such autonomous driving vehicles to estimate the location of BS and then aiding beamforming. Instead of BS broadcasting its location, this method allows smart vehicles with LIDAR to detect the location of BS through its LIDAR scans and complement this data with deep learning to reduce the search space for beamforming vectors.

The works mentioned above relies on additional resources such as GPS hardware to acquire location information, LIDAR hardware to acquire contextual information etc., for beam alignment. Even though all these solutions are able to present improved performance, additional hardware/resource requirements are a hindrance for widespread adoption of these solutions. Further, human aided acquisition of labeled dataset for training deep learning models severely limit the scalability

of the solutions.

Contributions. In this work, we propose a deep reinforcement learning [20], [21] based technique for blind beam alignment that does not need any additional hardware/resources and does not require any labeled dataset for training. The proposed method is designed to work in a scenario with multiple basestations as well as multiple UEs. By using the RF fingerprint of each UE produced by an omnidirectional beacon transmission, the system learns to predict the best BS to serve each UE as well as the beamforming vectors for each transmission. This makes the proposed solution also ideal for situations where UEs and environments are non-stationary since in such a case any contextual information obtained about the location alone may not be useful for beamforming.

Notations. Bold face lower-case letters (eg. \mathbf{x}) denote column vector and upper-case (eg. \mathbf{M}) denote matrices. Script face letters (eg. \mathcal{S}) denotes a set, $|\mathcal{S}|$ denotes the cardinality of the set \mathcal{S} . $f(\mathbf{x}; \boldsymbol{\theta})$ represents a function which takes in a vector \mathbf{x} and has parameters $\boldsymbol{\theta}$. A distribution with parameters $\boldsymbol{\theta}$ is represented as $p_{\boldsymbol{\theta}}(\cdot)$. \mathbb{E}_p is the expectation operator with respect to distribution p .

II. BLIND MMWAVE WAVE BEAM ALIGNMENT

We consider an mmWave MISO downlink scenario with multiple BSs trying to serve multiple UEs. Each base station has a small cell radius (hundreds of meters) within which it can serve and there exists a central base station (BS) that coordinates the cellular system. We assume that a reliable link exists between the micro basestations (μ BS) and the central BS which can ensure a robust exchange of data. For any additional signaling, we assume the existence of a dedicated control channel (CC). The aim is to select the best BS to serve each UE as well as the best set of beam alignment parameters for efficient beamforming. Also, we assume that all UEs use the same carrier frequency and hence the interference should also be reduced while selecting the beamforming parameters. All μ BS has a transmit power of P_{TX} .

A. Channel Model

Let N_{BS} represents the number of μ BS and N_{UE} represents the number of UEs. We consider a MISO system with N_T transmit antennas at each μ BS and $N_R = 1$ receive antenna at each UE. With single antenna UEs, have omnidirectional transmission. We consider a Uniform Planer Array (UPA) antenna at μ BS. The channel between the μ BS and UE is modeled based on the Saleh-Valenzuela channel model [22] for mmWave systems. The channel between the transmitter and receiver is given by

$$\mathbf{H} = \sqrt{\frac{N_T N_R}{L}} \sum_{l=1}^L \alpha_l \mathbf{a}_r(\phi_l^r, \theta_l^r) \mathbf{a}_t^*(\phi_l^t, \theta_l^t), \quad (1)$$

where L is the number of propagation paths, α_l is the complex gain associated with l^{th} path. (ϕ_l^t, θ_l^t) are the azimuth and elevation angles of departure of l^{th} ray at the μ BS respectively. Similarly, (ϕ_l^r, θ_l^r) are the angles of arrival of l^{th} ray at UE. We measure θ from $+z$ -axis and ϕ from $+x$ -axis. We assume the

μ BS UPA antenna is in yz -plane with $N_{t,h}$ and $N_{t,v}$ elements in y and z axis respectively and $N_t = N_{t,h} \times N_{t,v}$. The array response vector of transmitter, $\mathbf{a}_t(\phi, \theta)$, is given by

$$\mathbf{a}_t(\phi, \theta) = \frac{1}{\sqrt{N}} \left[1, \dots, e^{j \frac{2\pi}{\lambda} d(m \sin \phi \sin \theta + n \cos \theta)}, \dots, e^{j \frac{2\pi}{\lambda} d((N_{t,h}-1) \sin \phi \sin \theta + (N_{t,v}-1) \cos \theta)} \right]^T \quad (2)$$

where $0 < m < N_{t,h} - 1$ and $0 < n < N_{t,v} - 1$ and d is the inter-element spacing. Since we assume omni-directional reception with single antenna at the receiver, $\mathbf{a}^r(\phi, \theta) = 1$. The path loss (in dB) of mmWave propagation is modeled as [23],

$$PL(f, d)_{dB} = 20 \log_{10} \left(\frac{4\pi f}{c} \right) + 10n \left(1 + b \left(\frac{f - f_0}{f_0} \right) \right) \log_{10}(d) + X_{\sigma dB}, \quad (3)$$

where n is the path loss exponent, f_0 is the fixed reference frequency, b captures the frequency dependency of path loss exponent and $X_{\sigma dB}$ is the shadow fading term in dB .

The Signal to Interference Ratio (SINR) i^{th} UE which is having downlink transmission with j^{th} μ BS is given by

$$\gamma^i = \frac{P_{TX} |\mathbf{H}_{i,j} \mathbf{f}_j|^2}{\sum_{k=1, k \neq j}^{N_{BS}} P_{TX} |\mathbf{H}_{i,k} \mathbf{f}_k|^2 + \sigma^2}, \quad (4)$$

where $\mathbf{H}_{i,j}$ is the channel between i^{th} UE and j^{th} BS, \mathbf{f}_j is the transmit codeword used by μ BS and σ^2 is the noise power. The transmit codeword \mathbf{f}_j is computed from beamforming angles (ϕ_{ij}, θ_{ij}) as $\mathbf{f}_j = \mathbf{a}(\phi_{ij}, \theta_{ij})$ as given in (2).

RF signature of UE. Each UE transmits a uniquely identifiable beacon signal using omnidirectional transmission periodically during the time of downlink. All μ BS in the system can receive this uniquely identifiable signal. Since there may not exist direct pathways from the UE to BS for these beacon signals, the received power at each BS can have a complex relationship that is dictated by the scenario. However, with at least 4 μ BS used to construct the RF signature, it is possible to uniquely identify the location of origin of the signal. The final RF signature used by the learning system is a vector of N_{BS} dimensions, which is the received signal strength of the UE beacon signal at each of the N_{BS} micro basestations.

The learning problem is now to use the RF signatures along with the reported SINR values of each UE to predict which μ BS should serve which UE and with what values of ϕ and θ . An outline of the proposed procedure is given below.

- 1) Each UE send out a uniquely identifiable beacon signal using omnidirectional transmission.
- 2) Each μ BS receives the beacon signals transmitted by all the UEs. The the received power of beacon signals at each μ BS constitutes the RF signature for UEs.
- 3) Central basestation receives the RF signature collected by μ BS about each UE. Central basestation also obtains

the SINR from each UE about the ongoing downlink transmission.

- 4) Based on the RF signature and the SINR of each UE, the central basestation runs the proposed algorithm and selects best μ BS for each UE and the beam alignment angles.
- 5) Central basestation commands the selected μ BS to use the predicted angle parameters and serve particular UE.
- 6) Corresponding μ BS performs beam alignment based on the received command from central basestation for transmission until an update.

This process can be repeated every timestep or on an on-demand-manner to update the beam alignment process for each UEs. Compared to the standard procedure of beam sweeping, this can get the beam positioning in a single shot rather than searching for multiple combinations. Further, this method also enable the central basestation to choose the best μ BS for each UE based on realtime feedback.

III. LEARNING BASED BEAM ALIGNMENT

We model the problem as a Markov Decision Process (MDP) which comprises of a state space \mathcal{S} , an action space \mathcal{A} , an initial state distribution $p(s_1)$, a stationary distribution for state transition which obeys Markov property $p(s_{t+1}|s_t, a_t) = p(s_{t+1}|s_t, a_t, \dots, s_1, a_1)$ and a reward function $r: \mathcal{S} \times \mathcal{A} \rightarrow \mathbb{R}$. A policy π maps observed states to actions $\pi: \mathcal{S} \rightarrow \mathcal{A}$ and inturn obtains reward $r_t(s_t, a_t)$. An overview of the learning problem is depicted in Fig. 2.

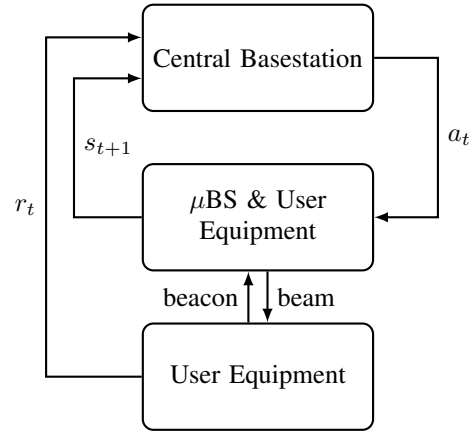


Fig. 2: Blind Beam alignment using DRL.

The input the learning agent is a $N_{UE} \cdot (N_{BS} + 1)$ dimensional vector where each consecutive $(N_{BS} + 1)$ elements corresponds to the receive SINR at UE with current beam alignment configuration and RF fingerprint (N_{BS} elements) from each μ BS about the UE. At each time step t , this constitutes the state described in the MDP ie., $s_t \in \mathbb{R}^{N_{UE} \cdot (N_{BS} + 1)}$. Action to be taken by the agent has to encode a discrete value referring to the index of the μ BS to serve each UE and also the (ϕ, θ) pair for the transmission. The reward at each time

instant t , r_t is taken as the mean rate achieved by the UEs at that instant is defined as,

$$r_t = \frac{1}{N_{UE}} \sum_{i=1}^{N_{UE}} \log_2(1 + \zeta_t^i), \quad (5)$$

where ζ_t^i is the instantaneous SINR at i^{th} UE.

A. Deep Reinforcement Learning

Reinforcement Learning (RL) [20] is a sub-class of artificial intelligence (AI) where the learning algorithm *interacts* with the *environment* to learn *optimal actions* which maximized a formulated *reward*. It differs from the Machine Learning (ML) paradigm in the way how samples are obtained for the learning process. While machine learning relies on labeled data to be fed into the algorithm for the learning process, reinforcement learning works by the learning agent itself acquiring the samples to improve its knowledge. While machine learning is ideal for scenarios where labeled data is available such as in classification and regression, and the prediction is not going to affect the future observations, reinforcement learning is used in scenarios where the learning agent is in control of the system whose output can change based on the agent's predictions. This difference also creates an *explore-exploit* behavior in RL algorithms where it is also required to explore unknown/less-known actions to acquire new samples.

In reinforcement learning, an agent is trained to optimize a policy π to increase the return $r_t(\gamma)$. The return $r_t(\gamma)$ is defined as the total discounted reward from the timestep t and can be expressed as $r_t(\gamma) = \sum_{t'=t}^{\infty} \gamma^{t'-t} r(s_{t'}, a_{t'})$, where $\gamma \in [0, 1]$. The discounting factor γ is used to capture the importance of future rewards in the current value estimate. With $\gamma \rightarrow 0$, the policy will become myopic and only considers current reward. With $\gamma \rightarrow 1$, the policy learns for long-term high reward. The objective of agent is to find a policy π which maximizes the expected cumulative discounted return $J(\pi) = \mathbb{E}[r_1(\gamma)|\pi]$. Agent computes the value function by a policy π for each state as the expected return from that state by following π , ie., $V^\pi(s) = \mathbb{E}[r_1(\gamma)|S_1 = s; \pi]$. Value of a state indicates how favorable each state is for the agent to be in. The quality of an action at each state is computed using Q-function as $Q^\pi(s, a) = \mathbb{E}[r_1(\gamma)|S_1 = s, A_1 = a; \pi]$ and indicates how good each action is to be taken from that state s . At each timestep, agent would take actions which maximizes the Q-value.

Deep Reinforcement Learning (DRL) [21] is the technique where deep an RL learning agent employs neural networks for facilitating the learning procedure. The function approximation capabilities of the neural networks are leveraged in DRL to map the observations to optimal actions. A neural network can be seen as a chain of functions that transforms its input to a set of outputs through a non-linear transform. In DRL, at each time step, after observing the state s , agent uses a neural network policy π to take an action a .

B. Deep Reinforcement Learning based Beam Alignment

The problem of beam alignment as formulated above is a challenging task for deep reinforcement learning as the action

space \mathcal{A} is a mixture of continuous (the value of angles) as well as discrete (the index to μBS) dimensions. Deep Deterministic Policy Gradient (DDPG) algorithm [24] is an actor-critic method for training deep reinforcement learning agents on continuous action domains. In this work, we chose to use DDPG as the learning algorithm to train DRL agent. As our problem has an action space which is a mix of discrete basestation selection and continuous beam alignment angles selection, we propose a novel neural network architecture that can handle pseudo-discrete and pure-continuous action spaces simultaneously for predicting actions.

Training the agent with DDPG. DDPG is based on the family of policy gradient algorithms in which the parameters of the policy are changed towards the direction of improvement of return. It is a two-step iterative process in which the policy is evaluated for the quality with current set of parameters and then, a policy improvement step updates the parameters in the ascent direction of maximum returns. DDPG has two neural networks: an actor network \mathbb{A} parameterized by ω^a which predicts the action a_t based on current state s_t and critic network \mathbb{C} parameterized by ω^c which computes the Q-value for the predicted action $Q(s_t, a_t)$. In order to get stable, uncorrelated gradients for policy improvement, DDPG maintains a replay buffer of finite size τ and sample the observations from the buffer in minibatches to update the parameters. DDPG also uses target networks with parameters $\bar{\omega}^a$ and $\bar{\omega}^c$ to avoid divergence in value estimation. At each timestep, the state s_i and the action takes a_i along with the reward obtained r_i and the next state s_{i+1} is stored as an experience (s_i, a_i, r_i, s_{i+1}) to the buffer \mathcal{B} . For training the actor and critic networks, N samples are taken from \mathcal{B} and is used to compute the gradients. For the critic network $\mathbb{C}(\omega^c)$ to compute the Q-value for each state action-pair, an estimate for return for state s_i in each sample is computed as

$$y_i = r_i + \gamma \mathbb{C}(s_{i+1}, \mathbb{A}(s_{i+1}|\bar{\omega}^a)|\bar{\omega}^c). \quad (6)$$

Based on the estimate for return, the Mean Squared Bellman Error (MSBE) is computed as

$$\mathcal{L} = \frac{1}{N} \sum_i (y_i - \mathbb{C}(s_i, a_i|\omega^c))^2. \quad (7)$$

Then, the critic network parameters are updated as

$$\omega^c \leftarrow \omega^c - \eta_c \nabla_{\omega^c} \mathcal{L}, \quad (8)$$

where $\eta_c \ll 1$ is the stepsize for stochastic update. For the actor network, the update depends on both the gradient of action as well as the improvement in Q-value. The final update for updating parameters of critic network ω^c is given by

$$\omega^a \leftarrow \omega^a + \eta_a \frac{1}{N} \sum_i (\nabla_{\omega^a} \mathbb{A}(s) \nabla_a \mathbb{C}(s, a)|_{a=\mathbb{A}(s)}), \quad (9)$$

where $\eta_a \ll 1$ is the update stepsize. Finally, the target network parameters are updated in every timestep to provide stable value estimates using an exponentially weighted update as

$$\bar{\omega}^c \leftarrow \lambda \omega^c + (1 - \lambda) \bar{\omega}^c; \quad \bar{\omega}^a \leftarrow \lambda \omega^a + (1 - \lambda) \bar{\omega}^a, \quad (10)$$

with $\lambda \ll 1$. Interested readers are directed to [24], [25] for more information.

Architecture of Neural Action predictor. DDPG is originally proposed for continuous action spaces. Since the problem of μBS selection is discrete and selecting (θ, ϕ) is continuous, a direct application of DDPG for the problem is impossible. Hence, we propose a novel architecture for neural function approximators which can be used for both discrete and continuous action spaces.

The proposed critic network \mathbb{C} is to predict the estimate the Q-value for each state-action pair. As Q-value is continuous, a traditional feedforward neural network with a scalar output can be used as \mathbb{C} , as used in DDPG. However, the actor network is responsible for predicting the best action a_t given a state s_t and the neural function approximator for \mathbb{A} needs to handle both discrete and continuous spaces. In the proposed architecture for actor network, we split the predictions for each UE through a sub-network at the output. All sub-networks share a common feature extractor which operates on the input to provide each UE sub-networks with a set of features that can be used to select the action corresponding to that UE. The architecture of proposed Neural Action Predictor is given in Fig. 3.

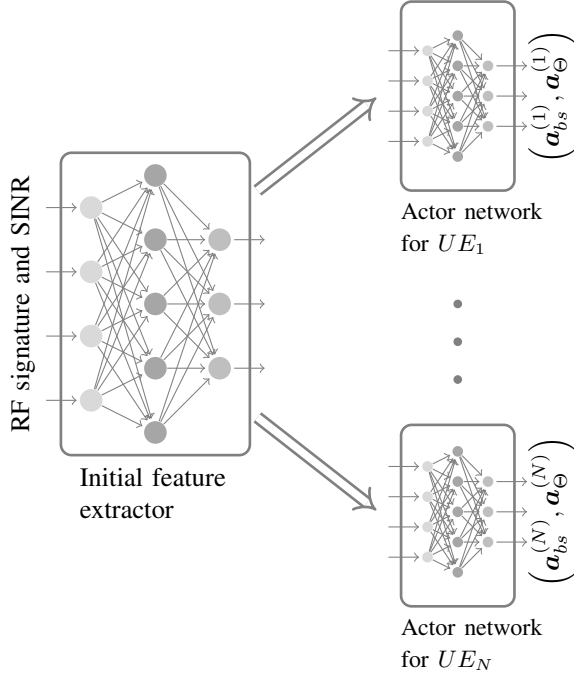


Fig. 3: Architecture of Proposed Neural Action Predictor.

At timestep t , let $\mathbf{x}_0 = s_t$ be the input to the common feature extractor network. We have $s_t \in \mathbb{R}^{N_{UE} \cdot (N_{BS} + 1)}$. The first L layers of the actor network constitute the common feature extractor network. At each layer, a linear combination of features from previous layer is created and is then passed through a non-linear activation function. Let $\mathbf{W}_l \in \mathbb{R}^{d_{l,o} \times d_{l,i}}$ and $\mathbf{b}_l \in \mathbb{R}^{d_{l,o}}$ be the weight and bias associated with layer l and $d_{l,i}$ and $d_{l,o}$ be the input and output dimensions of l^{th} layer. The output \mathbf{x}_l from l^{th} feature extractor layer is then computed as $\mathbf{x}_l = g(\mathbf{W}_l \mathbf{x}_{l-1} + \mathbf{b}_l)$, for $l = 1, \dots, L$

Algorithm 1 Proposed algorithm for μBS selection and beam alignment

- 1: **Parameters:** Set discounting factor γ , replay buffer size τ , number of episodes M , target update period U , update parameter λ , learning rates η_a and η_c .
- 2: Initialize the actor $\mathbb{A}(s|\omega^a)$ and the critic $\mathbb{C}(s, a|\omega^c)$ networks with random weights ω^a and ω^c respectively.
- 3: Initialize target networks with weights as $\bar{\omega}^a \leftarrow \omega^a$ and $\bar{\omega}^c \leftarrow \omega^c$.
- 4: Create an empty replay buffer $\mathcal{B} \leftarrow \{\}$ with size τ .
- 5: **for** episode = 1 . . . M **do**
- 6: Select a random valid action for each UE.
- 7: Observe SINR as well as the RF signature of each UE as state s_t .
- 8: **for** $t = 1 \dots T$ **do**
- 9: Set μBS and beam alignment angles for each UE according based on (11) and (12).
- 10: Get new state observation s_{t+1} .
- 11: Extract individual SINR for each UE from s_{t+1} and compute average rate as reward r_t given by (5).
- 12: Update replay buffer with experience as $\mathcal{B} \leftarrow \mathcal{B} \cup (s_t, a_t, r_t, s_{t+1})$.
- 13: **if** $|\mathcal{B}| \geq \tau$ **then**
- 14: Delete oldest experience from \mathcal{B} .
- 15: **end if**
- 16: Sample N experiences (s_i, a_i, r_i, s_{i+1}) from \mathcal{B} .
- 17: Compute return for each experience y_i .
- 18: Compute Mean Square Bellman Error as \mathcal{L} .
- 19: Update $(\omega^c, \bar{\omega}^c)$ and $(\omega^a, \bar{\omega}^a)$.
- 20: **end for**
- 21: **end for**

where $g(\cdot)$ is a non-linear activation function. The final set of extracted feature $\mathbf{x}_L \in \mathbb{R}^{d_L}$ is then fed to each of the sub-nets for action predictions for each UE.

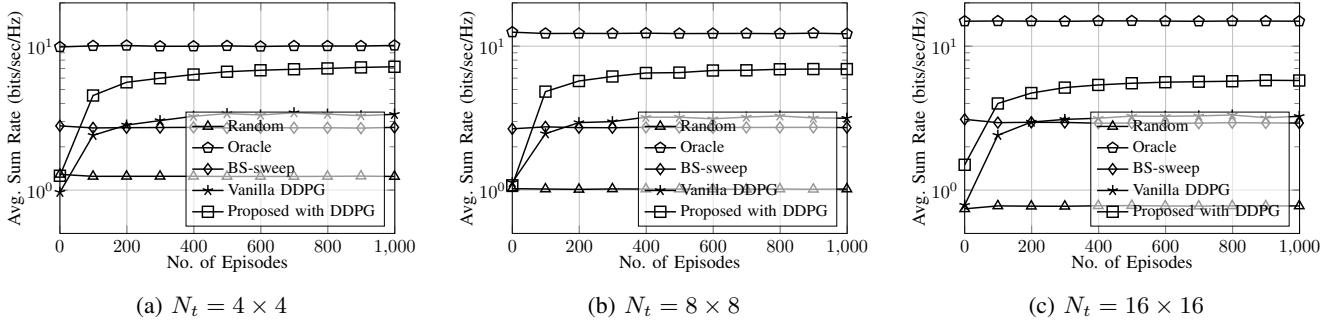
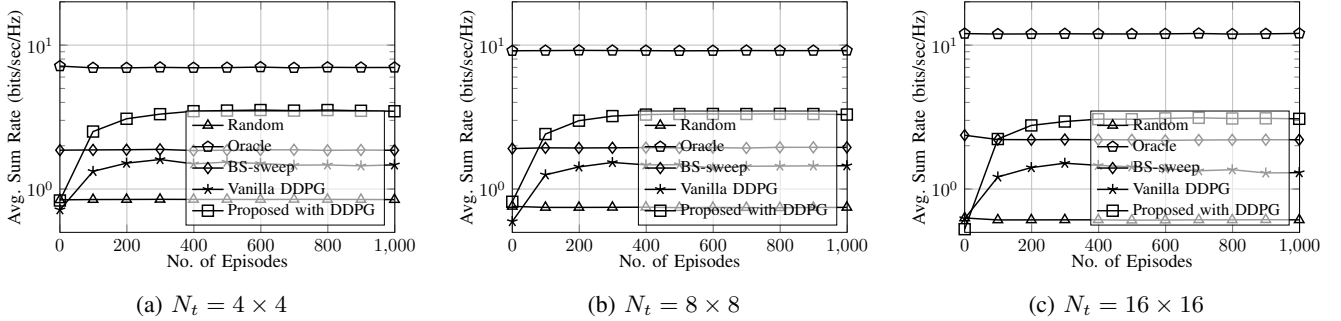
Actor sub-net for each UE uses a single layer for base station selection as most of the processing for μBS selection from input has been already done by the common feature extractor network. The actor sub-net for i^{th} UE predicts a normalized score over all the μBS indices using a softmax layer as

$$\mathbf{a}_{bs}^{(i)} = \text{softmax}(\mathbf{W}_{i,bs} \mathbf{x}_L + \mathbf{b}_{i,bs}), \quad (11)$$

where $\mathbf{W}_{i,bs} \in \mathbb{R}^{N_{BS} \times d_L}$ and $\mathbf{b}_{i,bs} \in \mathbb{R}^{N_{BS}}$. Then, the μBS to serve i^{th} UE is selected as basestation with highest normalized score in $\mathbf{a}_{bs}^{(i)}$.

Noting that the elevation angle and azimuth angles for beam alignment needs to depend both on information on the UE positions (available through \mathbf{x}_L) and the selected μBS for UE (available through $\mathbf{a}_{bs}^{(i)}$), we need a layer which can fuse together these information. For this, we first create a concatenating feature vector for each UE as $\mathbf{z}_i = [\mathbf{x}_L, \mathbf{a}_{bs}^{(i)}] \in \mathbb{R}^{d_L + N_{BS}}$. Then, the action corresponding to beam alignment angles for i^{th} UE are computed as

$$\mathbf{a}_{\Theta}^{(i)} = \tanh(\mathbf{W}_{i,\Theta} \mathbf{z}_i + \mathbf{b}_{i,\Theta}), \quad (12)$$

Fig. 4: Rate Evolution during learning for $N_{UE} = 3$.Fig. 5: Rate Evolution during learning for $N_{UE} = 5$.

where $\mathbf{W}_{i,\Theta} \in \mathbb{R}^{2 \times d_{L,o} + N_{BS}}$ and $\mathbf{b}_{i,\Theta} \in \mathbb{R}^2$. Note that the $\tanh(\cdot)$ activation function outputs values in range $[-1, +1]$ and hence $\mathbf{a}_{\Theta}^{(i)} \in [0, 1]^2$. Finally, the elevation and azimuth angles for beam alignment are computed (in radians) as $\theta_i = \frac{3\pi}{4} + \mathbf{a}_{\Theta}^{(i)}[1] \times \frac{\pi}{4}$, and $\phi_i = \mathbf{a}_{\Theta}^{(i)}[2] \times \frac{\pi}{2}$. The computation for elevation angle is based on the assumption that all UEs are below the height of μBS and hence $\theta_i \in [\pi/2, \pi]$. Similarly, it is assumed that $\phi_i \in [-\pi/2, +\pi/2]$.

The proposed algorithm to train the a DRL agent for the purpose of basestation selection and beam alignment is presented in Alg. 1.

IV. RESULTS

In this section, we provide simulation results for a four-junction scenario similar to [16] (extended to four roads) with $N_{BS} = 10$ and an intercell radius of approximately $100m$. A carrier frequency of $f_c = 28GHz$ is assumed and bandwidth of $5MHz$ is taken. All μBS are assumed to have UPA antenna of square dimensions with $N_t = 4 \times 4$ and with $d = \lambda/2$, where λ is the wavelength associated with frequency f_c . Following the Street Canyon configuration [23], we used $n = 1.98$, $\sigma = 3.1$, $b = 0$ and $f_0 = 1e9$ as the path loss parameters in (3). We provide results for $N_{UE} = 3, 5$, and 10 .

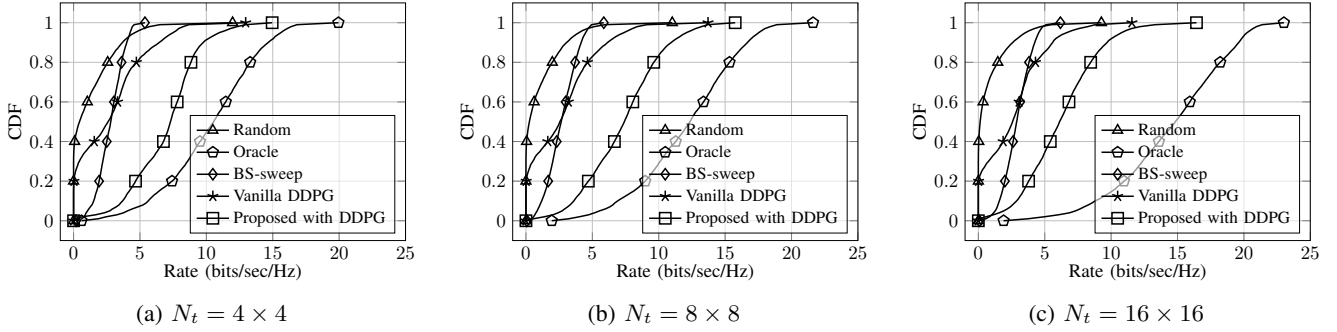
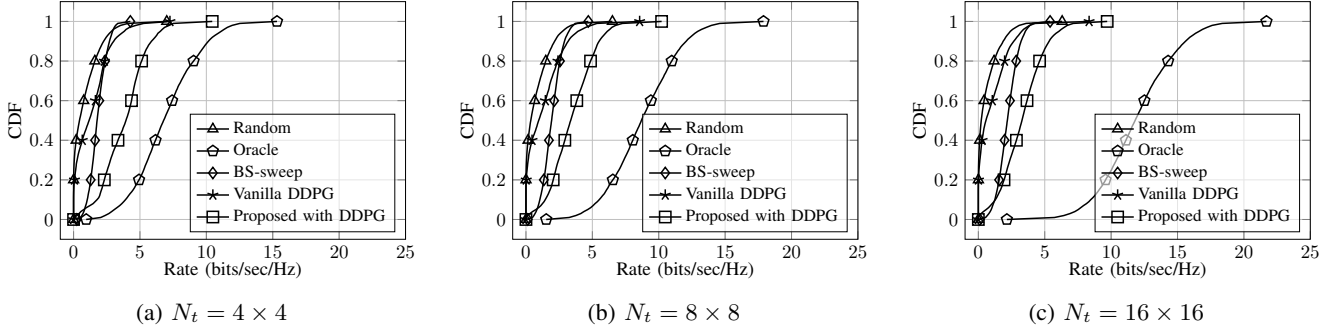
The performance of the following methods are discussed in this section:

1) **Random**: A blind agent which does not receive any inputs about the UEs, but tries to assign a μBS and a set of beam alignment angles for each UE. As this algorithm does not have any input/feedback, the rate obtained by this method is the minimum expected rate that can be obtained by any *intelligent* agent.

2) **Oracle**: This agent assumes that the exact knowledge about the location of UEs as well as the exact channel are known at the BS. Equipped with this information, *Oracle* picks the best μBS -UE assignment as well as the beam alignment angles. This is the maximum expected rate any algorithm can achieve.

3) **BS-Sweep**: This method is similar to the one proposed in [2]. However, as there are multiple μBS , all BS will simultaneously perform brute force beam search with a beam at every τ degrees. Since, some of the available time is spent on UE discovery process, the reported metrics are based on the available transmit time. Also, UE discovery needs to be performed at every instant as the UEs are mobile. We considered a frame period of $10ms$ and a beam scan period of $200\mu s$ per beam. While more number of beams increases the resolution of UE discovery, it also adds an overhead time. We provide results for $\tau = 5$ deg.

4) **Vanilla DDPG**: This is an RL agent which uses the feedforward neural network as proposed in [24] in the context of game-playing agents. This is provided to quantify the improvement in performance the proposed neural network architecture is providing. The neural network considered has with $L = 2$. Each hidden layer has 128 hidden nodes. The difference from the proposed method is the UE sub-net is absent in this method. For Q-value estimation, we consider a discounting factor of $\gamma = 0.60$, $\lambda = 0.001$ (found after sufficient hyper parameter tuning). We used Adam optimizer to update the neural network weights with $\eta_a = 0.0001$ and $\eta_c = 0.001$. We provide the results averaged over 5 agents, each trained for 1000 episodes. Each episode is

Fig. 6: CDF of observed rates for $N_{UE} = 3$.Fig. 7: CDF of observed rates for $N_{UE} = 5$.

considered 1000 timesteps long and the UE positions are reset at the end of each episodes.

- 5) **Proposed:** The proposed Deep Reinforcement Learning based agent has a feed forward critic network and UE sub-net augmented actor network, with $L = 2$. Each hidden layer has 128 hidden nodes. All other conditions including the training environment and the optimizer parameters are exactly same as *Vanilla DDPG* mentioned above.

The average sum rate evolution during the learning phase of proposed algorithm is given in Fig. 4 (for 3 UEs) and Fig. 5 (for 5 UEs) for different number of transmit antenna elements. With more number of antenna elements, the beam produced by UPA antenna becomes more narrower thus delivering most of the power towards the target direction. With less number of transmit antenna, the beams become broader and this can cause additional interference to neighboring UEs even with good spatial separation. This is evident from the trend of the average sum rate across different number of transmit elements. As the number of transmit elements in antenna increases, the SINR improves and we can see a improvement in the rate of oracle. Also, as the beams becomes narrower, the BS-Sweep method also improves the rate.

Also, the utility of the proposed architecture for Central node RL agent is evident from comparing the performance of *Vanilla DDPG* with simple feedforward network and *Proposed* method with per UE sub-net based function approximator.

In all the cases, the proposed method is able to give rates which are better than the BS-Sweep method. However, we can see that as the number of antenna elements increases the gap between the Proposed and the Oracle also increases,

even though the gap between oracle and BS-Sweep remains almost the same and that with random increases. The finer resolution of beams provided by the increased number of transmit elements also increases the effective search space for learning algorithm. As the search space increases, it is known that learning algorithms will incur difficulty in learning optimal actions. It remains to challenge see how this problem can be overcome through more focused training and better neural network architectures.

The cumulative distribution of rate achieved by each of the methods is given in Fig. 6 and Fig. 7. For each of the method, we ran the simulation for 10000 observations (10 episodes) and the data aggregated based on these observations are plotted. Note that the trained DRL-agents are used to get the rate distribution. Even though the DRL methods are able to give high rates compared to the baseline methods, as the dimensions of the problem increases, the gap between the proposed approach and the oracle also seems to increase. This again suggests that robust algorithms need to be developed to handle high dimensional learning problems.

V. CONCLUDING REMARKS

In this work, a deep reinforcement learning-based method for blind beamforming in mmWave communication systems is proposed for a multi-BS multi-UE scenario. The proposed method is shown to provide better data rates in mobile scenarios compared to traditional beam sweeping methods. This improved performance is achieved with almost no overhead to the system. The proposed neural network architecture for handling action spaces which are a mix of discrete and continuous actions is the key part of the improvement in perfor-

mance. Even though we showed results only with DDPG, the proposed neural architecture is agnostic to the policy gradient method and can be used with any other actor-critic methods. Further, the proposed neural architecture is also not limited to beamforming problem, but can be used in any problem where the action space is a mix of continuous and discrete actions.

REFERENCES

- [1] S. Kuttly and D. Sen, "Beamforming for millimeter wave communications: An inclusive survey," *IEEE Communications Surveys & Tutorials*, vol. 18, no. 2, pp. 949–973, 2015.
- [2] T. Nitsche, C. Cordeiro, A. B. Flores, E. W. Knightly, E. Perahia, and J. C. Widmer, "IEEE 802.11 ad: directional 60 GHz communication for multi-gigabit-per-second wi-fi," *IEEE Communications Magazine*, vol. 52, no. 12, pp. 132–141, 2014.
- [3] J. Zhang, Y. Huang, Q. Shi, J. Wang, and L. Yang, "Codebook design for beam alignment in millimeter wave communication systems," *IEEE Transactions on Communications*, vol. 65, no. 11, pp. 4980–4995, 2017.
- [4] T. Nitsche, A. B. Flores, E. W. Knightly, and J. Widmer, "Steering with eyes closed: mm-wave beam steering without in-band measurement," in *2015 IEEE Conference on Computer Communications (INFOCOM)*. IEEE, 2015, pp. 2416–2424.
- [5] F. Liu, P. Zhao, and Z. Wang, "EKF-based beam tracking for mmwave MIMO systems," *IEEE Communications Letters*, vol. 23, no. 12, pp. 2390–2393, 2019.
- [6] Y. LeCun, Y. Bengio, and G. Hinton, "Deep learning," *Nature*, vol. 521, no. 7553, p. 436, 2015.
- [7] C. Zhang, P. Patras, and H. Haddadi, "Deep learning in mobile and wireless networking: A survey," *IEEE Communications Surveys & Tutorials*, vol. 21, no. 3, pp. 2224–2287, 2019.
- [8] H. Ye, G. Y. Li, and B.-H. Juang, "Power of deep learning for channel estimation and signal detection in OFDM systems," *IEEE Wireless Communications Letters*, vol. 7, no. 1, pp. 114–117, 2018.
- [9] T. O'Shea and J. Hoydis, "An introduction to deep learning for the physical layer," *IEEE Transactions on Cognitive Communications and Networking*, vol. 3, no. 4, pp. 563–575, 2017.
- [10] V. Raj and S. Kalyani, "Backpropagating through the air: Deep learning at physical layer without channel models," *IEEE Communications Letters*, vol. 22, no. 11, pp. 2278–2281, 2018.
- [11] X. Gao, S. Jin, C.-K. Wen, and G. Y. Li, "ComNet: Combination of deep learning and expert knowledge in OFDM receivers," *IEEE Communications Letters*, vol. 22, no. 12, pp. 2627–2630, 2018.
- [12] H. Huang, W. Xia, J. Xiong, J. Yang, G. Zheng, and X. Zhu, "Unsupervised learning-based fast beamforming design for downlink MIMO," *IEEE Access*, vol. 7, pp. 7599–7605, 2018.
- [13] H. Huang, Y. Song, J. Yang, G. Gui, and F. Adachi, "Deep-learning-based millimeter-wave massive MIMO for hybrid precoding," *IEEE Transactions on Vehicular Technology*, vol. 68, no. 3, pp. 3027–3032, 2019.
- [14] X. Li and A. Alkhateeb, "Deep learning for direct hybrid precoding in millimeter wave massive MIMO systems," *arXiv preprint arXiv:1905.13212*, 2019.
- [15] Q. Wang and K. Feng, "Precodernet: Hybrid beamforming for millimeter wave systems using deep reinforcement learning," *arXiv preprint arXiv:1907.13266*, 2019.
- [16] A. Alkhateeb, S. Alex, P. Varkey, Y. Li, Q. Qu, and D. Tujkovic, "Deep learning coordinated beamforming for highly-mobile millimeter wave systems," *IEEE Access*, vol. 6, pp. 37 328–37 348, 2018.
- [17] K. Satyanarayana, M. El-Hajjar, A. Mourad, and L. Hanzo, "Deep learning aided fingerprint based beam alignment for mmwave vehicular communication," *IEEE Transactions on Vehicular Technology*, 2019.
- [18] A. Klautau, N. González-Prelcic, and R. W. Heath, "LIDAR data for deep learning-based mmwave beam-selection," *IEEE Wireless Communications Letters*, 2019.
- [19] M. Dias, A. Klautau, N. González-Prelcic, and R. W. Heath, "Position and LIDAR-aided mmwave beam selection using deep learning," in *2019 IEEE 20th International Workshop on Signal Processing Advances in Wireless Communications (SPAWC)*. IEEE, 2019, pp. 1–5.
- [20] R. S. Sutton and A. G. Barto, *Reinforcement learning: An introduction*. MIT press, 2018.
- [21] V. Mnih, K. Kavukcuoglu, D. Silver, A. A. Rusu, J. Veness, M. G. Bellemare, A. Graves, M. Riedmiller, A. K. Fidjeland, G. Ostrovski *et al.*, "Human-level control through deep reinforcement learning," *Nature*, vol. 518, no. 7540, p. 529, 2015.
- [22] O. El Ayach, S. Rajagopal, S. Abu-Surra, Z. Pi, and R. W. Heath, "Spatially sparse precoding in millimeter wave MIMO systems," *IEEE transactions on wireless communications*, vol. 13, no. 3, pp. 1499–1513, 2014.
- [23] "5G Channel Model for bands up to 100 GHz," Tech. Rep. October, 2016.
- [24] T. P. Lillicrap, J. J. Hunt, A. Pritzel, N. Heess, T. Erez, Y. Tassa, D. Silver, and D. Wierstra, "Continuous control with deep reinforcement learning," *arXiv preprint arXiv:1509.02971*, 2015.
- [25] D. Silver, G. Lever, N. Heess, T. Degris, D. Wierstra, and M. Riedmiller, "Deterministic policy gradient algorithms," 2014.